

# Symmetry-extended counting rules for periodic frameworks

S.D. Guest\*

Department of Engineering, University of Cambridge,  
Trumpington Street, Cambridge CB2 1PZ, UK

P.W. Fowler\*

Department of Chemistry, University of Sheffield,  
Sheffield S3 7HF, UK

October 25, 2013

## Abstract

A symmetry-adapted version of the Maxwell Rule appropriate to periodic bar-and-joint frameworks is obtained, and is further extended to body-and-joint systems. The treatment deals with bodies and forces that are replicated in every unit cell, and uses the point group isomorphic to the factor group of the space group of the framework. Explicit expressions are found for the numbers and symmetries of detectable mechanisms and states of self stress in terms of the numbers and symmetries of framework components. This approach allows detection and characterisation of mechanisms and states of self stress in microscopic and macroscopic materials and meta-materials. Illustrative examples are described. The notion of local isostaticity of periodic frameworks is extended to include point-group symmetry.

## 1 Introduction

Counting arguments give powerful conditions on rigidity/mobility of finite structures, and we consider here their applicability to extended periodic structures. Many objects in the macroscopic and microscopic worlds have been modelled as bar-and-joint frameworks, which consist of stiff bars connected with flexible joints (pin joints in 2D, spherical joints in 3D). Counting arguments for these frameworks were first formally expressed by Maxwell [1]. This rule, in the extension described by Calladine [2], is

$$\begin{aligned} (2D) \quad & m - s = 2j - b - 3 \\ (3D) \quad & m - s = 3j - b - 6 \end{aligned} \tag{1}$$

where  $m$  is the number of mechanisms,  $s$  the number of states of self-stress,

$j$  the number of joints, and  $b$  the number of bars of the framework. In this formulation, the constant terms on the RHS account for the rigid-body motions of the unsupported framework.

Scalar counting rules of this kind are powerful, but give limited information because they yield only the difference between the *numbers* of mechanisms and states of self-stress. The information content can be extended by considering the *symmetries* of the framework, and applying the counting approach symmetry by symmetry. Such an approach can reveal the existence of mechanisms and states of self stress which are hidden by cancellation within the bare scalar count. These extensions can be written compactly in terms of (typically reducible) *representations*  $\Gamma(\text{object})$  which collect the *characters*  $\chi_{\text{object}}(S)$  of sets of objects. For each symmetry operation  $S$ ,  $\chi_{\text{object}}(S)$  is the trace of the matrix that relates the set before and after application of  $S$ . For frameworks, the key representations are  $\Gamma(b)$  and  $\Gamma(j)$ , which describe the symmetries of bars and joints, respectively.

The symmetry-extended version of (1) is, from [3],

$$\Gamma(m) - \Gamma(s) = \Gamma(j) \times \Gamma_T - \Gamma(b) - \Gamma_T - \Gamma_R \quad (2)$$

where  $\Gamma_T$  and  $\Gamma_R$  are representations of relevant rigid-body translations and rotations, respectively. They are

$$\begin{aligned} (2D) \quad & \Gamma_T = \Gamma(T_x, T_y); \quad \Gamma_R = \Gamma(R_z), \\ (3D) \quad & \Gamma_T = \Gamma(T_x, T_y, T_z); \quad \Gamma_R = \Gamma(R_x, R_y, R_z), \end{aligned} \quad (3)$$

where the 2D restriction is to the  $(x, y)$  plane. A similar development can be framed for other models of structures: a finite body-and-joint framework also has a scalar counting rule for the net mobility [4, 5] and a symmetry extension of this counting rule has been derived [6].

Scalar counting can also be extended to periodic structures defined by a representative unit cell. This formulation, and its further extension to include symmetry, are the topics of the present paper. We show how the extended equations can be constructed for both pin-jointed and body-joint frameworks, and give some examples of their use. For pin-jointed periodic frameworks, Ross *et al.* [7] and Malestein and Theran [8] have previously considered counting for systems which are constrained to retain certain symmetries. Here, within a chosen periodicity, we effectively provide counts for all possible symmetries.

## 2 Counting for periodic bar-and-joint structures

The basis of our approach is consideration of the displacement and forces within the unit cell. The complete infinite structure is considered by translations of this cell. It is assumed here that the behaviour of the contents of the

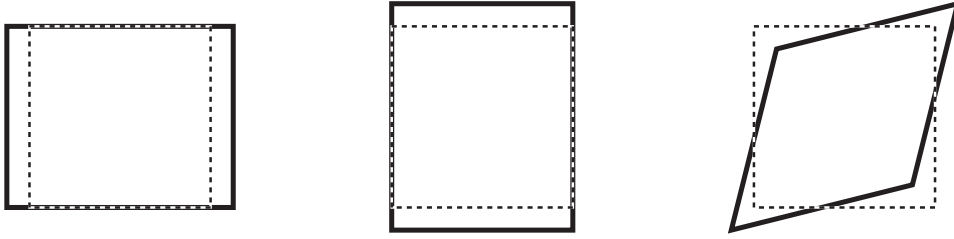


Figure 1: The deformations of the unit cell that are compatible with periodic mobility in 2D, comprising (left to right) two orthogonal stretches and one shear.

cell is also replicated by translation, i.e., we work in the  $k = 0$  wave-vector regime [9]. For these assumptions, Borcea and Streinu [10] give the extension of the scalar Maxwell counting rule for periodic structures. Here we give an alternative derivation that provides a basis for the further extension to include symmetry as described in Section 3.

A key element of the extension of rules (1) and (2) to repetitive periodic frameworks is the consideration of the appropriate rigid-body motions and deformations of the unit cell. Consider initially the affine infinitesimal deformations of a unit cell, used in solid mechanics to provide a basis for the strain tensor [11]. One basis for all possible deformations of the 2D unit cell (i.e., excluding rigid-body translations and rotations) is the set of the two orthogonal stretches in  $x$  and  $y$  directions, and the single  $xy$  shear (Figure 1). In 3D, a suitable basis for the possible deformations of the unit cell is the set of three orthogonal stretches (in  $x$ ,  $y$  and  $z$  directions) and three shears ( $xy$ ,  $yz$ ,  $zx$ ).

In periodic systems, the freedoms of the joints comprise the freedoms of each joint within the representative unit cell *plus* the deformations of the unit cell itself. Thus, the count of freedoms in 2D is  $2j + 3$ , and in 3D is  $3j + 6$ . However, this freedom includes rigid-body motions (two in 2D, three in 3D) that we wish to exclude from the list of mechanisms. Hence, the periodic equivalent of (2) is

$$\begin{aligned}
 (2D) \quad m - s &= 2j - b + 3 - 2 = 2j - b + 1 \\
 (3D) \quad m - s &= 3j - b + 6 - 3 = 3j - b + 3
 \end{aligned} \tag{4}$$

The RHS of (4) differs from the finite case (1) by addition of counts of 4 (2D) and 9 (3D), respectively. These equations can be derived more formally by considering the dimensions of the augmented compatibility matrix as described by Guest and Hutchinson [12].

A simple example system to illustrate the application of (4) is the kagome framework shown in Figure 2. With the given choice of smallest unit cell,

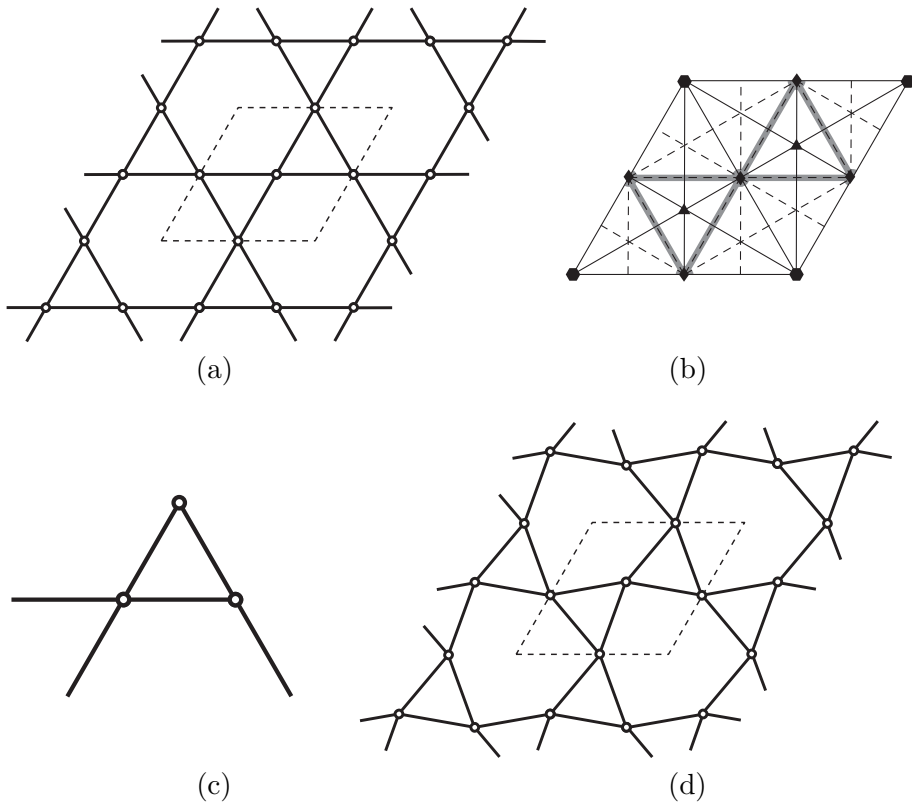


Figure 2: The kagome framework, showing (a) the choice of unit cell used here; (b) the unit cell with symmetry elements denoted by the standard symbols of a rhombus for a  $C_2$  axis, triangle for a  $C_3$  axis, hexagon for a  $C_6$  axis, solid line for a reflection line, and a dashed line for a glide line; (c) a motif with a minimal set of complete joints and bars; (d) a deformed configuration, illustrating the  $B_2$ -symmetric mechanism detected by the analysis reported in Section 4.1.

$j = 3$  and  $b = 6$ , where two of the joints lie on the unit cell boundary. The figure also shows what Owen and Power [13] call a ‘motif’ made up of complete joints and bars, disjoint copies of which recover the full kagome lattice by translation.

Except for systems which are *locally isostatic* [14], the result for  $m - s$  obtained from (4) will depend on the size of the unit cell chosen. Choosing a unit cell that is larger than the minimum unit cell effectively allows additional wave-vectors to be considered, beyond a  $k = 0$  wave-vector regime based on the minimum unit cell.

### 3 Counting with symmetry for periodic bar-and-joint structures

The symmetry group  $\mathcal{G}$  that describes a periodic framework is a *space group* (or, in 2D, a *plane group*). We consider the extension of the scalar approach of the previous section, where the target now is the description of the symmetries of the deformations and forces. Use of our previous assumption of replication of behaviour within the unit cell under translation implies that we do not have to deal with the infinite group  $\mathcal{G}$ , and instead we can restrict consideration to the *factor group*  $\mathcal{P} = \mathcal{G}/\mathcal{T}$ , where  $\mathcal{T}$  is the group of translations in the appropriate dimension. The factor group is isomorphic to a point group [15]. This fact allows us to capture interesting additional information regarding symmetry with an extension of the approach used for finite structures.

The scalar equation (4) for the net mobility  $m - s$  has terms relating to the freedom of the joints, the constraints imposed by the bars, the deformation modes of the unit cell, and rigid-body translations. The symmetry-extended version of this equation is

$$(2D, 3D) \quad \Gamma(m) - \Gamma(s) = \Gamma(j) \times \Gamma_T - \Gamma(b) + \Gamma_{\text{def}} - \Gamma_T \quad (5)$$

where the new term  $\Gamma_{\text{def}}$  collects the character of the infinitesimal deformations of the unit cell. These deformations can be described by a symmetric second-order tensor, and hence span the symmetry  $[\Gamma_T^2]$ , the symmetric part of the product  $\Gamma_T \times \Gamma_T$  [16]. As the antisymmetric part of the square is  $\{\Gamma_T^2\} = \Gamma_R$ , we have

$$(2D, 3D) \quad \Gamma_{\text{def}} = \Gamma_T \times \Gamma_T - \Gamma_R. \quad (6)$$

Hence the symmetry-extended Maxwell equation for periodic bar-and-joint frameworks is

$$(2D, 3D) \quad \Gamma(m) - \Gamma(s) = \Gamma(j) \times \Gamma_T - \Gamma(b) + \Gamma_T \times \Gamma_T - \Gamma_T - \Gamma_R. \quad (7)$$

with  $\Gamma_T$  and  $\Gamma_R$  defined for 2D and 3D as in (3), and all representations calculated in the factor group  $\mathcal{P}$ . This equation expresses our main result for periodic bar-and-joint frameworks in 2D and 3D. It gives an explicit expression for the numbers and symmetries of the mechanisms and states of self stress in terms of the numbers and symmetries of components of the framework.

Note that the rôle of the point group is somewhat different in the treatment of finite and periodic frameworks. In the finite case, the point group is the symmetry group of the object under consideration. In the periodic case, the point group arises only because it is isomorphic to the factor group. A corresponding element may therefore have a different physical significance

in each group. For example, in 2D there may be multiple centres of rotation and in 3D it may be that not all rotation axes pass through a common point. ‘Reflection’ operations of the point group may correspond to glide reflections in the factor group, and ‘rotations’ to screw rotations in the factor group.

In our examples, we will use Hermann-Mauguin notation for the space groups/plane groups, and Schoenflies notation for the point group isomorphic to the factor group, which we will often loosely call just ‘the point group’.

In general, the result for  $\Gamma(m) - \Gamma(s)$  obtained from (7) will depend on the size and location of the unit cell. Effectively, the choice of unit cell corresponds to a choice to work within a particular finite subgroup of the original infinite space group. We cannot tell in advance which choice of unit cell might lead to interesting behaviour; what we are doing here is to give the machinery for making the calculation once the unit cell is chosen. The system shown later in Figure 6 (analysed in Section 6) is an example where the correct choice of unit cell is important for the detection of a mechanism.

## 4 Examples for bar-and-joint frameworks

### 4.1 A 2D bar-and-joint framework: the kagome framework

The plane group of the kagome framework is  $p6m$ , and the point group isomorphic to the factor group is  $C_{6v}$  [15]. Simple counting gives  $2j - b + 1 = 1$ , indicating that the framework is locally isostatic [14], having at least one mechanism that repeats identically in every unit cell. Application of (7) in a tabular form showing the character under each symmetry operation, and using the Mulliken notation [17] for each representation, gives

$C_{6v}$	$E$	$2C_6$	$2C_3$	$C_2$	$3\sigma_v$	$3\sigma_d$	
$\Gamma(j)$	3	0	0	3	1	1	$A_1 + E_2$
$\times\Gamma_T$	2	1	-1	-2	0	0	$E_1$
=	6	0	0	-6	0	0	$B_1 + B_2 + 2E_1$
$-\Gamma(b)$	-6	0	0	0	-2	0	$-A_1 - B_1 - E_1 - E_2$
=	0	0	0	-6	-2	0	$-A_1 + B_2 + E_1 - E_2$
$+\Gamma_T^2$	4	1	1	4	0	0	$A_1 + A_2 + E_2$
$-\Gamma_T$	-2	-1	1	2	0	0	$-E_1$
$-\Gamma_R$	-1	-1	-1	-1	1	1	$-A_2$
$\Gamma(m) - \Gamma(s)$	1	-1	1	-1	-1	1	$B_2$

This tabulation, and those in the examples that follow, sets out the calculation in a standard form that was devised for [3] and used in subsequent papers. The general arrangement is similar to that used in chemical applications of point group theory, such as the calculation of symmetry properties of molecular vibrations [16, 18]. Some brief remarks about the notation may be useful. The first line gives the point group (denoted by the Schoenflies sym-

bol), and lists by classes the different symmetry operations that constitute the group. In general, operations  $S$  have symbols drawn from the set of:  $E$  for the identity,  $C_n$  for a proper rotation by  $2\pi/n$  (subscripted with prime(s) to avoid ambiguity when a  $C_2$  rotation is performed about an axis at right angles to the axis of highest order),  $i$  for the inversion,  $S_n$  for an improper rotation (a rotation through  $2\pi/n$  followed by a reflection in the plane perpendicular to the axis), and  $\sigma$  for reflection in a mirror plane (with a descriptive label such as  $v$ ,  $h$ ,  $d$  to distinguish vertical, horizontal, dihedral planes). Settings of the point groups and the definitions of the various distinguishing labels are given in, e.g., [16, 18, 19]. The final column of the table shows the reduction of the row of traces  $\chi(S)$  to a direct sum of irreducible representations of the point group. The notation for these follows Mulliken, as noted earlier: representations are labelled  $A$  (non-degenerate, symmetric under  $C_n$  rotation about the principal axis),  $B$  (non-degenerate, anti-symmetric under  $C_n$  rotation about the principal axis),  $E$  (doubly degenerate) or  $T$  (triply degenerate), and distinguished by subscripts and superscripts as necessary, such as  $g/u$  subscripts for symmetry/anti-symmetry under inversion, single and double prime superscripts for symmetry under horizontal planes, and so on. These standard labellings are to be found in compilations of character tables for chemistry [16, 19]

Returning to the specific example of the kagome framework: the calculation shown in the table above has identified the symmetry of the mechanism predicted by the scalar count. This mechanism has  $B_2$  symmetry. Note that the one-dimensional  $B_2$  representation (i) is present in only one copy in  $\Gamma(j) \times \Gamma_T$ ; (ii) is not present in  $\Gamma(b)$ ; and (iii) is not present in  $\Gamma_T^2 - \Gamma_R$ . Observations (a) and (b) imply that the mechanism is uniquely defined by the symmetry, and, by (c), does not require any deformation of the unit cell. The motion associated with the mechanism consists of alternating rotations of triangular units; the sense of rotation of any triangle is opposite to that of its three neighbours, as shown in Figure 2(d).

This example has illustrated the way that counting with symmetry can, in favourable cases, give not only the symmetry but also an explicit definition of the mechanism. In the particular case of the kagome lattice, the symmetry-detectable mechanism is known from numerical calculations to be unique under the constraint that the contents of all unit cells are defined by translation. Thus, the symmetry-extended Maxwell rule (12) gives a complete solution in this case.

## 4.2 A 3D bar-and-joint framework: the ‘sodalite’ framework

Sodalite is a dark blue mineral of formula  $\text{Na}_8\text{Cl}_2\text{Al}_6\text{Si}_6\text{O}_{24}$  [20] of space group  $P43n$  and point group  $T_d$ . The crystal structure is built from  $\text{SiO}_4$  and  $\text{AlO}_4$  tetrahedra, linked by corner-sharing of oxygen atoms. The experimentally observed structure can be considered to result from distortion of

a predecessor of higher symmetry by a process that was termed ‘rotational collapse’ by Pauling in his early studies of the X-ray diffraction pattern of this compound [21]. Concerted rotation of the tetrahedra is accompanied by small distortions in edge lengths and variations in rotational angle between chemically different tetrahedra [22].

For the present application, we will consider an idealised framework based on sodalite, in which the  $\text{MO}_4$  units are modelled as regular tetrahedra [23, 24]. In our bar-and-joint model, a bar is placed along each tetrahedron edge, and a spherical joint is placed at each tetrahedron vertex (oxygen position). Six bars meet at each joint, three from each of two neighbouring tetrahedra. We take all bars to have the same length, thereby removing the distinction between  $\text{SiO}_4$  and  $\text{AlO}_4$ , which raises the symmetry to  $I\bar{4}3m$  [25], which also has point group  $T_d$ . We now consider the fully expanded structure, which further raises the space group symmetry to the topological symmetry of the framework, i.e.,  $Im\bar{3}m$ , with point group  $O_h$ . With these restrictions, the framework is a model for the unsubstituted silica sodalite  $\text{Si}_{12}\text{O}_{24}$ , which does not occur naturally, but has been made by template synthesis [26, 27]. This is the ‘soda-1’ structure studied in [20]. The relationship between various sodalite-like frameworks has been described in [28]. The point group of our idealised structure (shown in Figure 3) is  $O_h$ . The unit cell contains 24 joints and 72 bars, and scalar counting using (4) gives  $m - s = 3$ . Application of (7) in tabular form is given in Table 1.

From the form of the reducible representation  $\Gamma(m) - \Gamma(s)$  in the final row of the table we can deduce that there are at least seven mechanisms that repeat identically in every unit cell, and that these span  $A_{2u} + T_{1g} + 2T_{2g}$ . Symmetry has clearly already revealed more mechanisms than the scalar count; it also gives an important clue to the deformation modes of this crystal framework. The non-degenerate  $A_{2u}$  mechanism breaks the inversion symmetry, and if we follow this distortion mode, we arrive at the space group  $I\bar{4}3m$  with point group  $T_d$ . In the lower group,  $\Gamma(m) - \Gamma(s) = A_1 + 2T_2 - 2A_2 - E$ ; in the absence of totally symmetric states of self stress, undetected in the higher symmetry group, the mechanism is finite [29] and becomes totally symmetric in the lower group. The mechanism consists of concerted rotations of tetrahedra, and follows the ‘rotational collapse’ mode described by Pauling [21], and this distortion of the model pin-jointed framework takes it close to the experimental structure of mineral sodalite. Although the mechanism follows a continuous geometric path, in practice it will ultimately be blocked by steric constraints of the kind invoked in more detailed descriptions of the crystal structure [20].

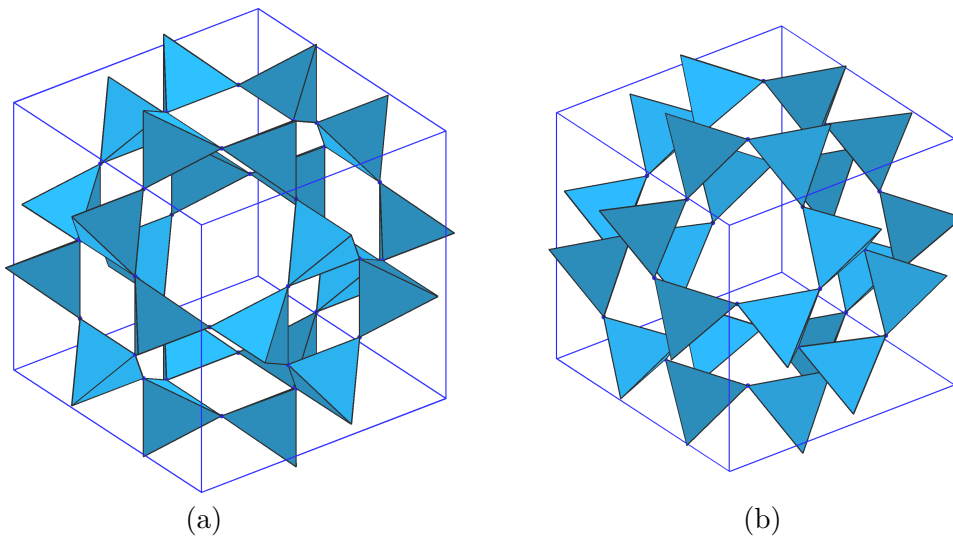


Figure 3: The ‘sodalite’ framework. Panel (a) shows the fully expanded maximum symmetry framework appropriate to the synthetic soda-1 structure. The unit cell used in the mobility calculation is indicated by thin lines, and for clarity the tetrahedra are shown as solid bodies. Panel (b) shows a deformed configuration of the framework which corresponds to the pure  $A_{2u}$  rotational collapse mode, and closely models the experimental structure of mineral sodalite. [20]. A rotation of  $23^\circ$  was applied to all tetrahedra in (a) to yield (b). This value is near to the average of the angles reported in [22] for  $\text{SiO}_4$  and  $\text{AlO}_4$  tetrahedra in the mineral; it leads to shrinkage of the side length of the unit cell by a factor of 0.92.

$O_h$	$E$	$8C_3$	$6C_2$	$6C_4$	$3C_4^2$	$i$	$6S_4$	$8S_6$	$3\sigma_h$	$6\sigma_d$	
$\Gamma(j)$	24	0	4	0	0	0	0	0	8	4	$2A_{1g} + 2E_g + 2T_{2g} + 2T_{1u} + 2T_{2u}$
$\times\Gamma_T$	3	0	-1	1	-1	-3	-1	0	1	1	$T_{1u}$
$=$	72	0	-4	0	0	0	0	0	8	4	$2A_{1g} + 2A_{2g} + 4E_g + 4T_{1g} + 4T_{2g} + 2A_{2u} + 2E_u + 6T_{1u} + 4T_{2u}$
$-\Gamma(b)$	-72	0	0	0	-8	0	0	0	-16	0	$-3A_{1g} - 3A_{2g} - 6E_g - 3T_{1g} - 3T_{2g} - A_{1u} - A_{2u} - 2E_u - 5T_{1u} - 5T_{2u}$
$=$	0	0	-4	0	-8	0	0	0	-8	4	$-A_{1g} - A_{2g} - 2E_g + T_{1g} + T_{2g} - A_{1u} + A_{2u} + T_{1u} - T_{2u}$
$+\Gamma_T^2$	9	0	1	1	1	9	1	0	1	1	$A_{1g} + E_g + T_{1g} + T_{2g}$
$-\Gamma_T$	-3	0	1	-1	1	3	1	0	-1	-1	$-T_{1u}$
$-\Gamma_R$	-3	0	1	-1	1	-3	-1	0	1	1	$-T_{1g}$
$\Gamma(m) - \Gamma(s)$	3	0	-1	-1	-5	9	1	0	-7	5	$A_{2u} + T_{1g} + 2T_{2g} - A_{2g} - E_g - A_{1u} - T_{2u}$

Table 1: Tabular calculation of  $\Gamma(m) - \Gamma(s)$  for the high-symmetry sodalite lattice illustrated in Figure 3(a).

## 5 Periodic mobility counting for body-and-joint models

In the analysis of finite structures, it is sometimes convenient to consider assemblies of bodies connected by joints rather than assemblies of joints connected by rigid bars. In the body-and-joint model, the rigid bodies are typically polygonal or polyhedral, and the joints may be of general type. This approach is also useful in the world of repetitive structures. Solid-state materials are often modelled in terms of rigid tetrahedral and octahedral units, see, for example, [30]. In the present section, we derive symmetry-extended counting rules for the mobility of periodic structures treated in this alternative body-and-joint model.

Scalar counting of the relative degrees of freedom, or mobility, of a mechanical linkage consisting of  $n$  bodies connected by  $g$  joints, where joint  $i$  permits  $f_i$  relative freedoms is [5, 6]

$$(2D) \quad m - s = 3(n - 1) - 3g + \sum_{i=1}^g f_i \tag{8}$$

$$(3D) \quad m - s = 6(n - 1) - 6g + \sum_{i=1}^g f_i$$

The terms on the RHS account respectively for the overall freedoms of all  $n$  bodies minus the rigid-body motions of the assembly, the constraints imposed by rigidly glued joints, and the restoration of the actual freedoms of the joints.

Conversion of (8) to allow for periodicity is straightforward. First, the rigid-body motions are restored, then the freedoms associated with the deformations of the unit cell are added, and finally the appropriate rigid-body displacements are removed. The net effect is to add four to the RHS of the 2D equation, and nine to the RHS of the 3D equation, as for the pin-jointed case (4), leaving, for periodic systems,

$$(2D) \quad m - s = 3n - 3g + \sum_{i=1}^g f_i + 4 \tag{9}$$

$$(3D) \quad m - s = 6n - 6g + \sum_{i=1}^g f_i + 9$$

For 2D periodic linkages where all joints are pin joints, we have  $f_i = 1$  for all  $i$ , and for 3D periodic linkages where all joints are spherical joints we have  $f_i = 3$  for all  $i$ , and hence (9) becomes

$$\begin{aligned}
(2D) \quad & m - s = 3n - 2g + 1 \\
(3D) \quad & m - s = 6n - 3g + 3
\end{aligned} \tag{10}$$

In the symmetry extension of the mobility criterion for finite frameworks it is useful to consider the ‘contact polyhedron’  $C$ , which has vertices that represent the rigid elements of the structure and has edges that represent the joints. The expression is derived from a thought experiment where the structure is first considered to be a rigid assembly with all joints glued, and the joint freedoms are then restored. The result is, from [6],

$$(2D, 3D) \quad \Gamma(m) - \Gamma(s) = (\Gamma(v, C) - \Gamma_{\parallel}(e, C) - \Gamma_0) \times (\Gamma_T + \Gamma_R) + \Gamma_{\text{freedoms}} \tag{11}$$

where now  $\Gamma(v, C)$  is the permutation representation of the vertices of  $C$ ,  $\Gamma_{\parallel}(e, C)$  is the representation of the set of vectors directed along the edges of  $C$ , and  $\Gamma_{\text{freedoms}}$  is the representation of the freedoms of the joints. The detailed structure of  $\Gamma_{\text{freedoms}}$  depends on the types and distributions of the joints. Conversion of (11) for periodic structures follows the same route as the extension of (2) to (7), i.e., addition of the same 4-fold (2D)/9-fold (3D) reducible representations  $\Gamma_T \times \Gamma_T$  to the RHS, leaving, for periodic systems,

$$(2D, 3D) \quad \Gamma(m) - \Gamma(s) = (\Gamma(v, C) - \Gamma_{\parallel}(e, C) - \Gamma_0) \times (\Gamma_T + \Gamma_R) + \Gamma_{\text{freedoms}} + \Gamma_T \times \Gamma_T \tag{12}$$

with  $\Gamma_T$  as given in (3). The contact ‘polyhedron’ is now infinite, but we consider its restriction to the unit cell, or more formally its quotient with respect to translations.

Specialisation to the case of all pin joints (2D) or all spherical joints (3D) relies on [6]

$$(2D, 3D) \quad \Gamma_{\text{freedoms}} = \Gamma_{\parallel}(e, C) \times \Gamma_R \tag{13}$$

and hence the explicit formula for periodic structures of this simplified type is

$$(2D, 3D) \quad \Gamma(m) - \Gamma(s) = \Gamma(v, C) \times (\Gamma_T + \Gamma_R) - \Gamma_{\parallel}(e, C) \times \Gamma_T + \Gamma_T \times \Gamma_T - \Gamma_T - \Gamma_R \tag{14}$$

where the three terms on the RHS encapsulate the freedoms, constraints and periodicity effects that contribute to the net mobility of the structure.

## 6 Examples for body-and-joint structures

The kagome and sodalite calculations of Section 4 can be reworked in terms of rigid triangular plates and rigid tetrahedral bodies. The results for  $\Gamma(m) - \Gamma(s)$  from (14) for any particular system will be identical to those from the bar-and-joint analysis using (7). This correspondance is guaranteed by the presence of rigid simplices of bars within the bar-and-joint version of the framework.

### 6.1 Infinite frameworks of pin-jointed rectangles

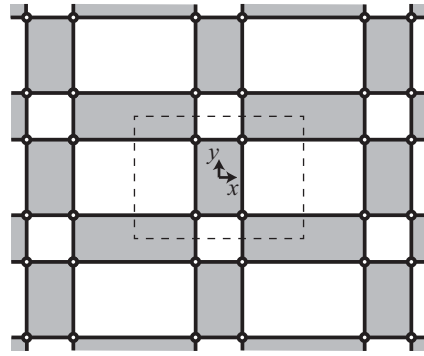
The body-and-joint mobility criterion (14) is ideally suited to analysis of the hinged polygon constructions that are common in the literature of auxetic materials [e.g., 31, 32]. One system that has been studied in detail in connection with the explanation of auxetic behaviour in 2D is built on the square lattice. Symmetry calculations on three variants of this basic system are treated here.

The first model [32] consists of a lattice of rectangles of two sizes, pinned together at their corners. In the highest-symmetry realisation this structure belongs to the plane group  $p2mm$  with point group  $C_{2v}$ . The calculation using (14) with the unit cell shown in Figure 4 is

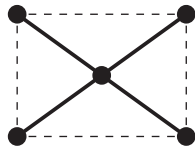
$C_{2v}$	$E$	$C_2$	$2\sigma_x$	$2\sigma_y$	
$\Gamma(v, C)$	2	2	2	2	$2A_1$
$\times(\Gamma_T + \Gamma_R)$	3	-1	-1	-1	$A_2 + B_1 + B_2$
=	6	-2	-2	-2	$2A_2 + 2B_1 + 2B_2$
$-\Gamma_{\parallel}(e, C)$	-4	0	0	0	$-A_1 - B_1 - E_1 - B_1$
$\times\Gamma_T$	2	-2	0	0	$B_1 + B_2$
=	-8	0	0	0	$-2A_1 - 2A_2 - 2B_1 - 2B_2$
$\Gamma_T^2 - \Gamma_R$	1	5	1	1	$2A_1 + A_1 - B_1 - B_2$
$\Gamma(m) - \Gamma(s)$	-1	3	-1	-1	$A_2 - B_1 - B_2$

Scalar counting (10) gives  $m - s = -1$ , showing only that the system is overconstrained. The symmetry calculation reveals that the net count of  $-1$  conceals one mechanism and two states of self stress. Further, the  $A_2$  mechanism is finite in the absence of an equisymmetric state of self stress, as a necessary consequence of the abelian nature of  $C_{2v}$ . As Grima *et al.* [32] comment, this mechanism is auxetic.

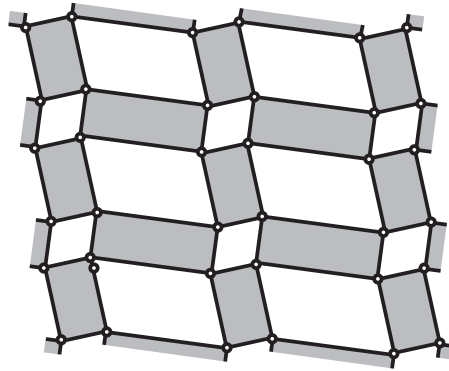
In the case where the rectangles degenerate to squares of two different sizes, we recover the system considered by Grima and Evans [31]. The plane group is now  $p4mm$  and the point group is  $C_{4v}$  with mirror lines  $d$  running both vertically and horizontally in the (now square) unit cell, and the mir-



(a)



(b)



(c)

Figure 4: Model for an auxetic material based on rectangles of two sizes, showing (a) the model and the choice of unit cell with rigid plates indicated by shading; (b) the contact polyhedron  $C$  for the unit cell; (c) a deformed configuration, illustrating the  $A_2$ -symmetric mechanism.

ror lines  $v$  running diagonally. In this case, construction of a bar-and-joint model consistent with the symmetry would require each square to be braced across both diagonals, generating an unwanted local state of self-stress. This is avoided for the body-and-hinge model, for which the symmetry calculation gives

$C_{4v}$	$E$	$2C_4$	$C_2$	$2\sigma_v$	$2\sigma_d$	
$\Gamma(v, C)$	2	2	2	2	2	$2A_1$
$\times(\Gamma_T + \Gamma_R)$	3	1	-1	-1	-1	$A_2 + E$
=	6	2	-2	-2	-2	$2A_1 + 2 + 2E$
$-\Gamma_{\parallel}(e, C)$	-4	0	0	-2	0	$-A_1 - B_1 - E$
$\times\Gamma_T$	2	0	-2	0	0	$E$
=	-8	0	0	0	0	$-A_1 - A_2 - B_1 - B_2 - 2E$
$\Gamma_T^2 - \Gamma_R$	1	-1	5	1	1	$A_1 + B_1 + B_2 - E$
$\Gamma(m) - \Gamma(s)$	-1	1	3	-1	-1	$A_2 - E$

Clearly the scalar count (10) is unchanged by the symmetrization of the rectangles, and the only change in  $\Gamma(m) - \Gamma(s)$  is the collapse of the  $B_1$  and  $B_2$  pair of states of self-stress to a degenerate  $E$  pair. The physical conclusions about the continuous nature of the mechanism are unchanged.

In the further limiting case when the two squares become equal in size, a smaller unit cell becomes possible, as shown in Figure 5. Straightforward application of (14) gives

$C_{4v}$	$E$	$2C_4$	$C_2$	$2\sigma_v$	$2\sigma_d$	
$\Gamma(v, C)$	1	1	1	1	1	$A_1$
$\times(\Gamma_T + \Gamma_R)$	3	1	-1	-1	-1	$A_2 + E$
=	3	1	-1	-1	-1	$A_1 + A_2 + E$
$-\Gamma_{\parallel}(e, C)$	-2	0	2	0	0	$-E$
$\times\Gamma_T$	2	0	-2	0	0	$E$
=	-4	0	-4	0	0	$-A_1 - A_2 - B_1 - B_2$
$\Gamma_T^2 - \Gamma_R$	1	-1	5	1	1	$A_1 + B_1 + B_2 - E$
$\Gamma(m) - \Gamma(s)$	0	0	0	0	0	0

Thus, in this case, neither the scalar count nor the symmetry count gives any indication of the mobility that we know to be present from the previous calculation. The physical explanation of this apparent paradox is clear; by assumption of the smaller unit cell, we have constrained every square to

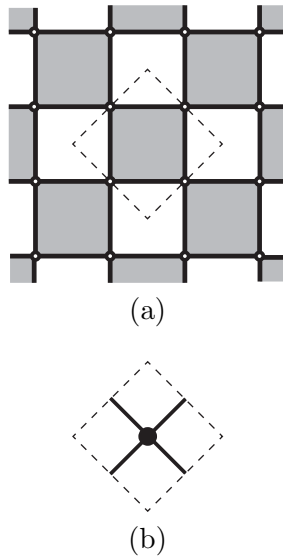


Figure 5: Model for an auxetic material based on squares of equal size, showing (a) the model and the smallest choice of unit cell with rigid plates indicated by shading; (b) the contact polyhedron  $C$  for the unit cell which in this case consists of a single unique vertex.

behave in the same way, and this is inconsistent with the counter-rotating nature of the mechanism.

This example illustrates the potential pitfalls of fixing a unit cell in advance. Mechanisms will only be discovered by this method if they break symmetry and are consistent with a fixed unit cell. Figure 6 shows twelve different unit cells, each of which may give different results for  $\Gamma(m) - \Gamma(s)$ , reflecting the different states of self-stress and mechanisms that are consistent with the subgroup of the space group that is implied by the choice of unit cell.

## 7 A symmetry-extended notion of local isostaticity

An isostatic framework is one that has neither mechanisms nor states of self stress. A necessary scalar condition for isostaticity is  $m - s = 0$ , which is the character under the identity of the stronger condition  $\Gamma(m) - \Gamma(s) = 0$  which demands cancellation under all symmetry operations [33]. For periodic systems this condition is impossible to attain [12], but Kapko *et al.* [14] introduced the concept of ‘locally isostatic’ to denote situations where, on average, the number of constraints balance out the number of freedoms. Hence for a locally isostatic 2D periodic framework,  $b - 2j$  and  $m - s = 1$

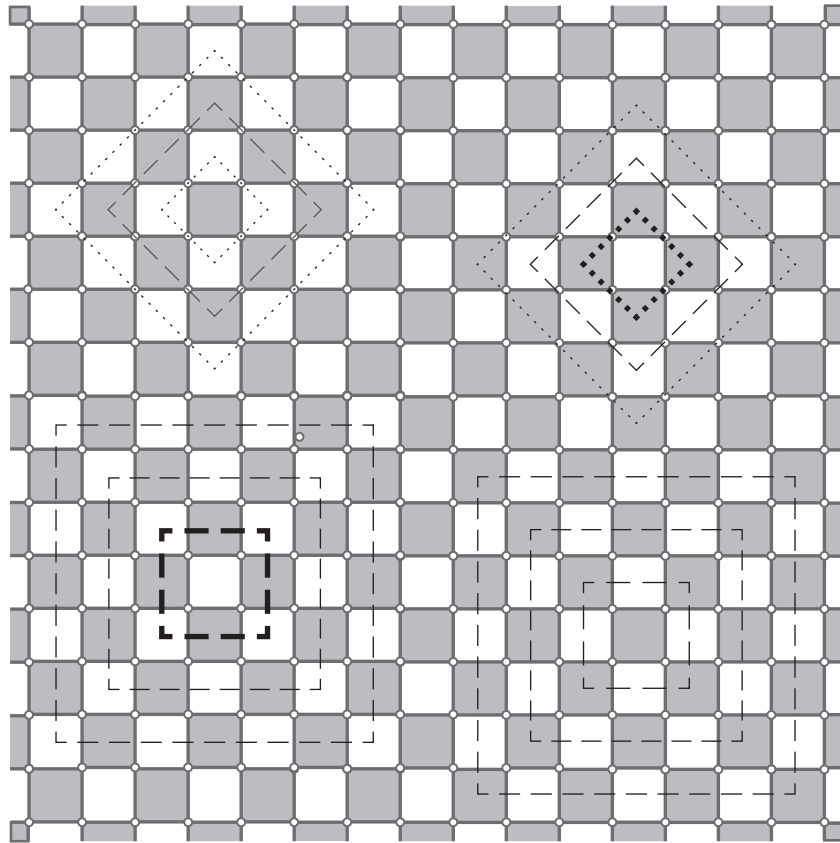


Figure 6: Twelve different choices of unit cell for an auxetic material based on squares of equal size. The unit cells marked with dotted (rather than dashed) lines are inconsistent with the mechanism in which alternate squares rotate in opposite directions. The two unit cells marked in bold are analysed by tabular calculation in the text.

by (4). The equality  $b = 2j$  (equivalently,  $b = 3j$  in 3D) is again effectively the character under the identity of a symmetry relationship,

$$\Gamma(b) = \Gamma(j) \times \Gamma_T. \quad (15)$$

Suppose that we insist that (15) holds, i.e., that  $\chi_b(R) = \chi_j(R)\chi_T(R)$  for all  $R$ . Then, by (7),

$$\Gamma(m) - \Gamma(s) = \Gamma_T \times \Gamma_T - \Gamma_T - \Gamma_R, \quad (16)$$

which is a stronger symmetry condition for an extended notion of local isostaticity. In 2D, (16) leads to some interesting conclusions about the possible placement of structural components of the periodic framework. The conditions for the vanishing of the character of  $\Gamma(m) - \Gamma(s)$  for the different allowed operations  $R$  are, in 2D:

$$\begin{aligned} \chi(E) : & & 2j &= b \\ \chi(C_2) : & & -2j_2 &= b_2 \\ \chi(C_3) : & & -j_3 &= b_3 \\ \chi(C_4) : & & 0j_4 &= b_4 \\ \chi(C_6) : & & j_6 &= b_6 \\ \chi(\sigma) : & & 0j_\sigma &= b_\sigma \end{aligned} \quad (17)$$

where  $b_N$  and  $j_N$  are, respectively, the number of bars and joints lying on a  $C_N$  axis, and  $b_\sigma$  and  $j_\sigma$  are, respectively, the number of bars and joints preserved by a  $\sigma$  mirror. As each of these counts is non-negative, we can deduce that  $j_2 = j_3 = 0$ ,  $b_2 = b_3 = b_4 = b_\sigma = 0$ . Further, as no bar can be preserved by a  $C_N$  operation with  $N > 2$ ,  $b_6 = 0$  and hence  $j_6 = 0$ . Also, as any joint on a  $C_4$  axis must also lie on a  $C_2$  axis,  $j_2 \geq j_4$  and as  $j_2 = 0$ ,  $j_4$  must also be 0. The value of  $j_\sigma$  is unrestricted. Hence, a 2D locally isostatic periodic framework with  $j$  joints and  $2j$  bars may have joints only in general position or in mirror lines, and all bars must be in general position. If all joints are also in general position, we have

$$\Gamma_j = \frac{j}{|G|} \Gamma_{\text{reg}}; \quad \Gamma_b = \frac{2j}{|G|} \Gamma_{\text{reg}} \quad (18)$$

where  $|G|$  is the order of the point group, and  $\Gamma_{\text{reg}}$  is the regular representation, with  $\chi_{\text{reg}}(E) = |G|$ , and  $\chi_{\text{reg}}(R) = 0$  for  $R \neq E$ ; trivially,  $\Gamma_j \times \Gamma_T - \Gamma(b) = 0$  in this case.

There is a distinction between scalar and symmetry-extended notions of local isostaticity. The latter is more restrictive, and may depend on the choice of unit cell. For instance, the kagome lattice is 4-regular, and hence has  $m - s = 1$ . However, the symmetry calculation with the minimum unit

cell used in (Section 4.1) gives

$$\begin{aligned}\Gamma(j) \times \Gamma_T - \Gamma(b) &= (B_1 + B_2 + 2E_1) - (A_1 + B_1 + E_1 + E_2) \\ &= -A_1 + B_2 + E_1 - E_2.\end{aligned}\tag{19}$$

in the  $C_{6v}$  point group. The operations for which the framework departs from the local isostatic count are  $R = C_2$ , where  $j_2 = 3$ , and the mirror  $\sigma$  where  $b_\sigma = 1$ . Once the system has distorted along the  $B_2$  mode, the plane group is reduced to  $p31m$  with point group  $C_{3v}$  and the RHS of (19) vanishes. Only then has the system attained locally isostatic status on both scalar and symmetry-extended criteria. Considered in terms of characters in the distorted configuration, as the mirror lines run parallel with the bars, but pass through joints and hexagon centres,  $b_\sigma = 0$  and  $j_\sigma = 2$ . In addition, the  $C_3$  axes lie at the centres of triangles and hexagons, and hence  $j_3 = b_3 = 0$ , consistent with (17). Indeed, in this case, for any unit cell consisting of  $n \times n$  copies of the one shown in Figure 2(d), the counts will become  $b_\sigma = 0$ ,  $j_3 = b_3 = 0$ , with  $j_\sigma = 2n$ , showing that the distorted kagome lattice with space group  $p31m$  is locally isostatic for any choice of unit cell.

## Acknowledgements

We would like to thank Holger Mitschke (Universität Erlangen-Nürnberg) for helpful discussions during the drafting of this paper. PWF thanks the Royal Society and Leverhulme Trust for a Senior Research Fellowship.

## References

- [1] Maxwell, J. C., 1864 On the calculation of the equilibrium and stiffness of frames. *Philosophical Magazine*. **27**, 294–299.
- [2] Calladine, C. R., 1978 Buckminster Fuller’s “Tensegrity” structures and Clerk Maxwell’s rules for the construction of stiff frames. *International Journal of Solids and Structures* **14**, 161–172.
- [3] Fowler, P. W. and Guest, S. D., 2000 A symmetry extension of Maxwell’s rule for rigidity of frames. *International Journal of Solids and Structures* **37**, 1793–1804.
- [4] Grübler, M., 1917 *Getriebelehre*. Berlin: Springer.
- [5] Kutzbach, K., 1929 Mechanische leitungsverzweigung. *Maschinenbau, Der Betrieb* **8**, 710–716.
- [6] Guest, S. D. and Fowler, P. W., 2005 A symmetry-extended mobility rule. *Mechanism and Machine Theory* **40**, 1002–1014.

- [7] Ross, E., Schulze, B. and Whiteley, W., 2011 Finite motions from periodic frameworks with added symmetry. *International Journal of Solids and Structures* **48**(11–12), 1711–1729. ISSN 0020-7683. doi: 10.1016/j.ijsolstr.2011.02.018.
- [8] Malestein, J. and Theran, L., 2012 Generic rigidity with forced symmetry and sparse colored graphs. *ArXiv e-prints* ArXiv:1203.0772 [math.GT].
- [9] Dove, M. T., 2005 *Introduction to Lattice Dynamics*. Cambridge University Press.
- [10] Borcea, C. S. and Streinu, S., 2010 Periodic frameworks and flexibility. *Proceedings of the Royal Society A: Mathematical, Physical and Engineering Science* **466**, 2633–2649.
- [11] Timoshenko, S. P. and Goodier, J. N., 1969 *Theory of elasticity*. McGraw-Hill, third edition.
- [12] Guest, S. D. and Hutchinson, J. W., 2003 On the determinacy of repetitive structures. *Journal of Mechanics and Physics of Solids* **51**(3), 383–391.
- [13] Owen, J. C. and Power, S. C., 2011 Infinite bar-joint frameworks, crystals and operator theory. *New York Journal of Mathematics* **17**, 445–490.
- [14] Kapko, V., Treacy, M. M. J., Thorpe, M. F. and Guest, S. D., 2009 On the collapse of locally isostatic networks. *Proceedings of the Royal Society A: Mathematical, Physical and Engineering Science* **465**, 3517–3530.
- [15] Burns, G. and Glazer, A. M., 1990 *Space groups for solid state scientists*. Academic Press, second edition.
- [16] Atkins, P. W., Child, M. S. and Phillips, C. S. G., 1970 *Tables for Group Theory*. Oxford University Press.
- [17] Mulliken, R. S., 1955 Report on notation for the spectra of polyatomic molecules. *Journal of Chemical Physics* **23**(11), 1997–2011.
- [18] Bishop, D. M., 1973 *Group Theory and Chemistry*. Oxford: Clarendon Press.
- [19] Altmann, S. L. and Herzig, P., 1994 *Point-Group Theory Tables*. Oxford: Clarendon Press.

- [20] Thomson, K. T., Wentzcovitch, R. M., McCormick, A. and Davis, H. T., 1998 A density functional study of sodalite: a new view on an old system. *Chemical Physics Letters* **283**, 39–43.
- [21] Pauling, L., 1930 The structure of sodalite and helvite. *Zeitschrift für Kristallographie* **74**, 213–225.
- [22] Hassan, I. and Grundy, H. D., 1984 The crystal structures of sodalite-group minerals. *Acta Crystallographica B* **40**, 6–13.
- [23] Sartbaeva, A., Wells, S., Treacy, M. M. J. and Thorpe, M. F., 2006 The flexibility window in zeolites. *Nature Materials* **5**, 962–965.
- [24] Power, S. C., 2013 Polynomials for crystal frameworks and the rigid unit mode spectrum. Submitted for publication,.
- [25] Depmeier, W., 1992 Remarks on symmetries occurring in the sodalite family. *Zeitschrift für Kristallographie* **199**, 75–89.
- [26] Bibby, D. M. and Dale, M. P., 1985 Synthesis of silica-sodalite from non-aqueous systems. *Nature* **317**, 157–158.
- [27] Richardson, J. W., Jr., Pluth, J. J., Smith, J. V., Dytrych, W. J. and Bibby, D. M., 1988 Conformation of ethylene glycol and phase change in silica sodalite. *Journal of Physical Chemistry* **92**, 243–247.
- [28] Fischer, R. X. and Baur, W. H., 2009 Symmetry relationships of sodalite (SOD)-type crystal structures. *Zeitschrift für Kristallographie* **224**, 185–197.
- [29] Guest, S. D. and Fowler, P. W., 2007 Symmetry conditions and finite mechanisms. *Journal of Mechanics of Materials and Structures* **2**(2), 293–301.
- [30] Giddy, A. P., Dove, M. T., Pawley, G. S. and Heine, V., 1993 The determination of rigid-unit modes as potential soft modes for displacive phase transitions in framework crystal structures. *Acta Crystallographica Section A* **49**, 697–703.
- [31] Grima, J. N. and Evans, K. E., 2000 Auxetic behaviour from rotating squares. *Journal of Materials Science Letters* **19**, 1563–1565.
- [32] Grima, J. N., Manicaro, E. and Attard, D., 2011 Auxetic behaviour from connected different-size squares and rectangles. *Proceedings of the Royal Society A: Mathematical, Physical and Engineering Science* **467**, 439–458.
- [33] Connelly, R., Fowler, P. W., Guest, S. D., Schulze, B. and Whiteley, W. J., 2009 When is a symmetric pin-jointed framework isostatic? *International Journal of Solids and Structures* **46**, 762–773.